Collaborative Enhancement of Endothelial Targeting of Nanocarriers by Modulating Platelet-Endothelial Cell Adhesion Molecule-1/CD31 Epitope Engagement

Ann-Marie Chacko,[†,‡,▽] Jingyan Han,[§,▽] Colin F. Greineder,[§] Blaine J. Zern,[§] John L. Mikitsh,[†] Madhura Nayak,[†] Divya Menon,[§] Ian H. Johnston,[#] Mortimer Poncz,[#] David M. Eckmann,[∥] Peter F. Davies,[⊥] and Vladimir R. Muzykantov*[,‡,§]

[†]Department of Radiology, Division of Nuclear Medicine and Clinical Molecular Imaging, [‡]Center for Targeted Therapeutics and Translational Nanomedicine, Institute for Translational Medicine and Therapeutics, [§]Department of Systems Pharmacology and Translational Therapeutics, [∥]Department of Anesthesiology & Critical Care, [⊥]Department of Pathology and Institute for Medicine and Engineering, Perelman School of Medicine, University of Pennsylvania, Philadelphia, Pennsylvania 19104, United States and [#]Department of Pediatrics, Division of Hematology, The Children's Hospital of Philadelphia, Philadelphia, Pennsylvania 19104, United States. [▽]These authors contributed equally to this work.

ABSTRACT Nanocarriers (NCs) coated with antibodies (Abs) to extracellular epitopes of the transmembrane glycoprotein PECAM (platelet endothelial cell adhesion molecule-1/CD31) enable targeted drug delivery to vascular endothelial cells. Recent studies revealed that paired Abs directed to adjacent, yet distinct epitopes of PECAM stimulate each other's binding to endothelial cells *in vitro* and *in vivo* ("collaborative enhancement"). This phenomenon improves targeting of therapeutic fusion proteins, yet its potential role in targeting multivalent NCs has not been addressed. Herein, we studied the effects of Ab-mediated collaborative enhancement on multivalent NC spheres coated with PECAM Abs (Ab/NC, ~180 nm diameter). We found that PECAM Abs do mutually enhance endothelial cell binding of Ab/NC coated by paired, but not "self" Ab. *In vitro*, collaborative enhancement of endothelial binding of Ab/NC by paired Abs is modulated by Ab/NC avidity, epitope selection, and flow. Cell fixation, but not blocking of endocytosis, obliterated collaborative enhancement of Ab/NC binding, indicating that the effect is mediated by molecular reorganization of PECAM molecules in the endothelial plasmalemma. The collaborative enhancement of Ab/NC binding was affirmed *in vivo*. Intravascular injection of paired Abs enhanced targeting of Ab/NC to pulmonary vasculature in mice by an order of magnitude. This stimulatory effect greatly exceeded enhancement of Ab targeting by paired Abs, indicating that '"collaborative enhancement"' effect is even more pronounced for relatively large multivalent carriers *versus* free Abs, likely due to more profound consequences of positive alteration of epitope accessibility. This phenomenon provides a potential paradigm for optimizing the endothelial-targeted nanocarrier delivery of therapeutic agents.

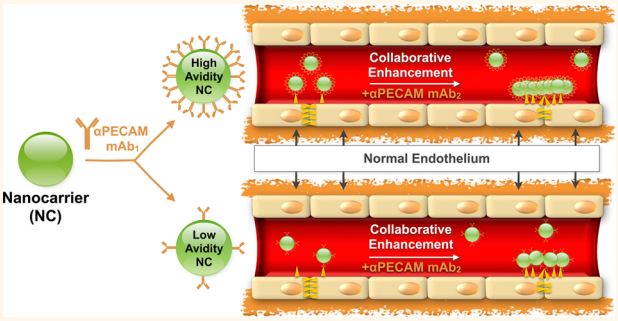

KEYWORDS: nanocarrier · targeted drug delivery · PECAM-1 · multivalent interactions · collaborative enhancement

Targeting drugs using nanocarriers (NCs) is a promising yet challenging area of nanomedicine.[1−4] Carriers offer numerous advantages including high payload and its isolation *en route*, multivalent anchoring, and intracellular delivery, but also face difficult translational issues, necessitating mechanistic studies of their targeting. Binding to target cells is different for free affinity ligands (e.g., antibodies (Abs) or their fragments) *versus* carriers coated with the same ligand molecules.[5−7] Complex dynamics of such affinity interactions are governed by specific features of both carrier design such as ligand surface density and of the target cell and molecule such as its accessibility and conformation in plasma membrane.[8]

* Address correspondence to muzykant@mail.med.upenn.edu.

Received for review October 6, 2014 and accepted July 8, 2015.

Published online July 08, 2015
10.1021/nn505672x

Targeting drugs to endothelial cells (ECs) has the potential to improve management of diseases involving ischemia, inflammation, thrombosis, and tumor growth.[9−16] In particular, the surface of carriers coated with Abs to the cell adhesion molecule PECAM (platelet endothelial cell adhesion molecule 1, PECAM-1, CD31) enables endothelial delivery of NCs, improving therapeutic effects of their drug cargoes in animal models.[17−21] These encouraging results justify further optimization of endothelial targeting and effect of anti-PECAM/NC (indicated as Ab/NC unless indicated otherwise). PECAM, a 130 kDa transmembrane glycoprotein of the Ig-superfamily, is stably expressed on the surface of ECs, preferentially at cell−cell borders,[22,23] and mediates interactions of leukocytes with endothelium.[24−26]

Targeting to PECAM is modulated by selection of the anchoring epitopes. For example, anchoring of nanocarriers coated by anti-PECAM Abs to distinct PECAM epitopes results in different rates of endothelial endocytosis and intracellular trafficking of Ab/NC.[27] Furthermore, functional effects of Abs to distinct PECAM epitopes differ in terms of the influence of homologous PECAM−PECAM interactions between adjacent endothelial cells or/and adhering leukocytes.[26,28]

We recently discovered that paired anti-PECAM Abs to adjacent yet distinct epitopes on PECAM increased each other's binding to endothelium,[29] a counterintuitive finding since steric hindrance might be expected to inhibit binding. Alternatively, this "collaborative enhancement" of endothelial targeting by the paired Abs may be attributable to increased accessibility of the epitopes for the stimulated antibody due to conformational changes in the target molecule induced by the stimulating antibody. Collaborative enhancement of targeting may also have important practical biomedical implications. For example, paired antibodies boost endothelial targeting[29] and the therapeutic effect[30,31] of a protein drug fused with a scFv directed to an adjacent PECAM epitope.

Here we have investigated the effect of the paired anti-PECAM Ab on targeting Ab/NC and report that paired antibodies stimulate the endothelial targeting of Ab/NC directed to the first and second Ig domains of PECAM (i.e., IgD1 and IgD2).

RESULTS AND DISCUSSION

Collaborative Enhancement of Endothelial Binding of Ab/NC by Paired Ab: Effects of Flow, Epitope Selection, Ab/NC Avidity, and Cellular Status. Employing a live-cell system of human umbilical vein endothelial cells (HUVECs), we studied mutual effects of paired anti-PECAM Abs on endothelial binding of Ab/NC variably coated with approximately 50 or 200 Ab molecules per spherical particle (final diameter of ∼180 nm). Binding characteristics of monoclonal Abs to distinct epitopes in IgD1 in human PECAM, Ab62 and Ab37 (Ab_{1h} and Ab_{2h}, respectively), and in IgD2 in mouse PECAM, Ab 390 and Ab Mec13 (Ab_{1m} and Ab_{2m}) are shown in Table S1.[29]

Ab_{1h}/NC, but not control IgG/NC, bound to static EC proportionally to low and high Ab surface density (Figure 1), consistent with previous studies.[32,33] Preincubation with an excess of the same soluble Ab_{1h} (i.e., "self") inhibited endothelial binding of Ab_{1h}/NC, whereas pretreatment with control IgG ("solo") had no effect. In contrast, pretreatment with Ab_{2h} to a second distinct epitope ("paired") enhanced binding of Ab_{1h}/NC most significantly for high density Ab/NC (Figure 1B; $P < 0.001$).

Therefore, "paired" Ab_{2h} enhances binding of Ab_{1h}/NC, similarly to its effect on binding of free Ab_{1h}, likely *via* increasing accessibility of the Ab_{1h} epitope.[29] However, unlike "collaborative binding" of free Ab_{1h} and Ab_{2h}, no enhancement was observed at simultaneous coincubation of "paired" Ab_{2h} with Ab_{1h}/NC; pretreatment with paired Ab_{2h} is required to

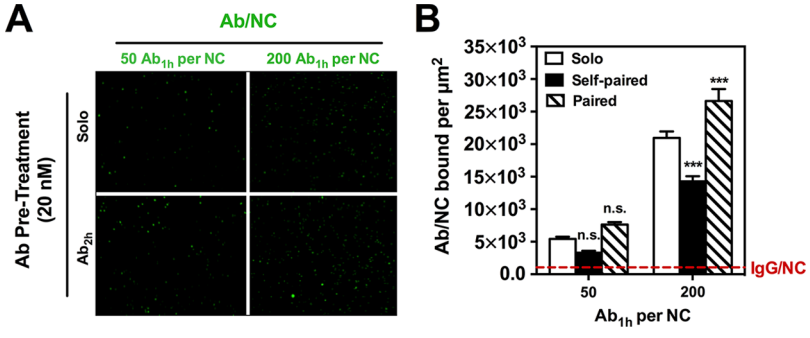

Figure 1. Free paired Ab_{2h} preincubation specifically enhances endothelial cell (EC) binding of anti-PECAM Ab_{1h}/NCs at low and high Ab densities. (A) Representative fluorescence images showing that HUVEC binding of green fluorescent NCs having 25% surface coating with Ab_{1h} (*i.e.*, 50 Ab/particle) or fully coated with Ab_{1h} (*i.e.*, 200 Ab/particle) was increased when EC were preincubated with free paired Ab_{2h} (20 nM) for 30 min compared with solo IgG pretreatment (20 nM). (B) EC binding of Ab_{1h}/NC at low and high Ab density over particle surface (50 Ab/NC and 200 Ab/NC, respectively) with solo IgG (open bars) was inhibited by self-paired free Ab_{1h} (filled bars) and significantly enhanced by paired free Ab_{2h} (hashed bars) at high Ab density. The EC binding of fluorescent particles in each image field (10^4 μm^2), as quantified by fluorescence microscopy, was represented as Ab/NC bound per μm^2. Dashed line represents total binding of nontargeted IgG-coated NCs. Data are mean ± SE ($n = 8$). n.s., $P > 0.05$; ***, $P < 0.001$.

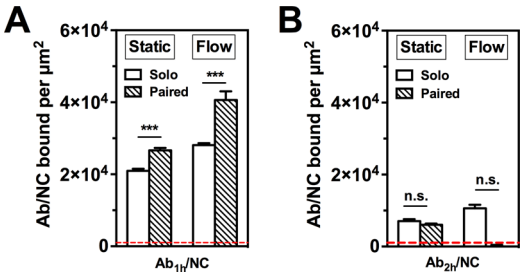

Figure 2. Fluid shear stress potentiates endothelial binding of anti-PECAM Ab_{1h}/NC induced by paired Ab_{2h} incubation. Under static and flow conditions (4 dyn/cm^2), paired Ab_{2h} preincubation (20 nM) significantly enhanced endothelial binding of Ab_{1h}/NCs (200 Abs/NC) (A), whereas paired Ab_{1h} had no effect on endothelial binding of Ab_{2h}/NCs (200 Abs/NC) (B). The number of EC bound Ab_{1h}/NCs was quantified in each fluorescence image field (10^4 μm^2); dashed line indicates nonspecific binding of fully coated control IgG/NC. Data are shown as mean ± SE (n = 8). ***, $P < 0.001$; n.s., $P > 0.05$. Open bars show NC binding with solo treatment; hashed bars show NC binding with paired free Ab treatment.

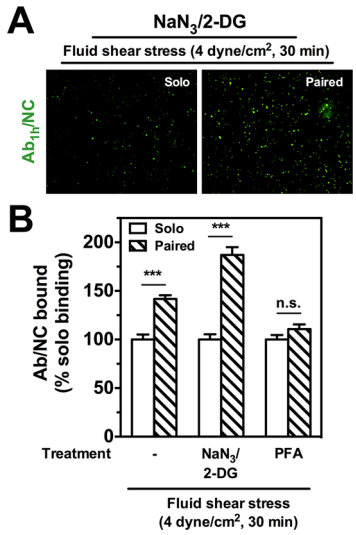

Figure 3. Blocking internalization does not abrogate stimulated endothelial binding of anti-PECAM Ab_{1h}/NCs. (A) Under flow conditions of acute fluid shear stress (4 dyn/cm^2, 30 min), fluorescence images show endothelial HUVEC binding of Ab_{1h}/NCs (green) with paired Ab_{2h} pretreatment (20 nM) is increased compared to solo IgG pretreatment with NaN_3/2-DG (5 mM). (B) Despite blocking of internalization with NaN_3/2-DG, Ab_{1h}/NC binding is significantly increased by 87% over solo binding under flow. For cells prefixed with paraformaldehyde (PFA, 1%, 10 min) and then subjected to flow, the enhanced endothelial binding of Ab_{1h}/NCs (200 Abs/NC) with free Ab_{2h} preincubation (20 nM) is completely abolished to control IgG levels. The number of EC bound fluorescent particles in each image filed (10^4 μm^2) was quantified by fluorescence microscopy under flow conditions and presented as % solo binding. Data are mean ± SE (n = 8). n.s., $P > 0.05$. Open bars show NC binding with solo treatment; hashed bars show NC binding with paired free Ab treatment.

stimulate Ab_{1h}/NC binding (Supporting Information, Figure S1). Apparently, Ab_{1h}/NCs have faster binding kinetics than relatively small free Ab_{1h}; hence, Ab_{2h}-mediated exposure of the secondary Ab_{1h} PECAM epitope must precede the administration of Ab/NCs. This is not necessary for free Abs.

To increase the physiological relevance of the model, we studied effects of Ab_{2h} on the binding of Ab_{1h}/NC to endothelial cells under acute flow. We found that flow (i) stimulates "solo" Ab_{1h}/NC binding and (ii) potentiates the collaborative enhancement of Ab_{1h}/NC binding by paired Ab_{2h} pretreatment (Figure 2). The latter was a somewhat unexpected finding, the specific mechanisms of which merit separate investigation. Here we explored two potential means by which flow might influence the collaborative enhancement of NC binding. First, the distribution of PECAM on HUVEC was examined under static conditions, after short-term (30 min) exposure to flow, and following overnight flow adaption. In contrast to a prominent change in the distribution of filamentous actin (F-actin), no effect was seen on the localization of PECAM, which remained predominantly at cell−cell junctions (Supporting Information, Figure S3). Second, we investigated endocytosis of Ab_{1h}/NC bound to PECAM, a process recently shown to be modulated by flow.[32−35] We found that collaborative enhancement of Ab_{1h}/NC binding to endothelial cells under flow was unaffected when internalization was blocked *via* ATP-depletion with sodium azide/2-deoxyglucose (NaN_3/2-DG) (Figure 3A,B). In contrast, paraformaldehyde (PFA)-fixation of cells completely abrogated the effect of pretreatment with paired Ab_{2h} (Figure 3C). Since both methods effectively block endocytosis of Ab_{1h}/NC (Figure S3), these results suggest that it may be conformational flexibility and lateral diffusion[36,37] of PECAM molecules, eliminated by PFA but not NaN_3/2-DG, which may be critical for the collaborative enhancement effect.

Under physiologic conditions, individual factors such as flow and nanocarrier avidity, are likely to both influence the magnitude of the collaborative enhancement effect in complex ways. For example, under flow conditions, pretreatment with Ab_{2h} resulted in a significant increase in Ab_{1h}/NC binding only at higher density of targeted anti-PECAM antibody (Supporting Information, Figure S4). As mentioned above, the details of these interactions and their underlying mechanisms deserve separate investigation; in the context of this study, it suffices to say that the observed effects of flow were encouraging in terms of the potential physiological relevance of the collaborative enhancement effect and motivated the animal studies shown in the following sections.

It is important to note that the paired enhancement effect is not necessarily mutual. In our initial report of the collaborative enhancement effect, we found that while Ab_{2h} significantly enhanced the binding of Ab_{1h}, Ab_{1h} had no effect on the binding of free Ab_{2h}. This was different from the paired mouse anti-PECAM antibodies (Ab_{1m} and Ab_{2m}), where the effect was mutual; that is, each antibody enhanced the binding of the other.[29] Consistent with this previous result, we found

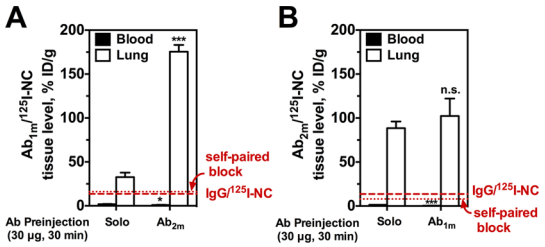

Figure 4. *In vivo* endothelial targeting of Ab/^{125}I-NC to muPECAM is enhanced by paired muPECAM Ab. (A) Lung tissue activity of Ab_{1m}/^{125}I-NC (200 μg NC per mouse) at 30 min p.i. is enhanced significantly with paired Ab_{2m} (30 μg for 30 min) as compared to IgG preinjection. Blood levels of Ab_{1m}/^{125}I-NC following paired Ab treatment are lower than blood in IgG pretreated mice. (B) Lung tissue activity of Ab_{2m}/^{125}I-NC (200 μg NC per mouse) is increased nonsignificantly with paired Ab_{1m} (30 μg for 30 min), whereas blood levels following paired Ab treatment are significantly lower than blood levels in IgG pretreated mice. Dashed line indicates lung uptake of nonspecific IgG/^{125}I-NC and dotted line is Ab_{1m}/^{125}I-NC or Ab_{2m}/^{125}I-NC lung uptake blocked with respective self-paired Ab pretreatment. Data represented as mean ± SE (n = 3−9 mice per group). ***, $P < 0.001$; n.s., $P > 0.05$.

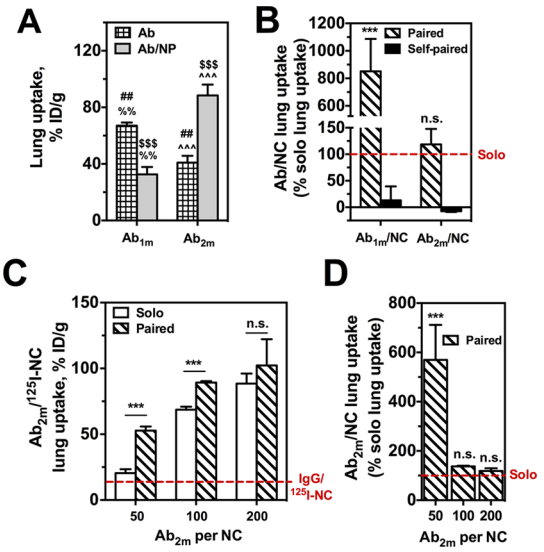

Figure 5. Paired Ab enhancement of anti-PECAM nanocarrier lung targeting is dependent on epitope accessibility and nanocarrier avidity. (A) Pulmonary uptake of PECAM-targeted free anti-PECAM ^{125}I-Abs (Ab_{1m} and Ab_{2m}) *versus* fully coated Ab/^{125}I-NC show differential binding depending on muPECAM epitope accessibility once Ab is immobilized on NC. Crossed and open bars show vascular-targeted binding with solo treatment for free Ab or NC, respectively. (#) Comparison of free Ab_{2m} to free Ab_{1m}; (%) comparison of free Ab_{1m} to Ab_{1m}/NC; ($) comparison of Ab_{1m}/NC to Ab_{2m}/NC; (∧) comparison of free Ab_{2m} to Ab_{2m}/NC. ##, %%, $P < 0.01$; $$$, ∧∧∧, $P < 0.001$. (B) Preinjection of paired Abs differentially stimulated lung uptake of fully coated Ab/NCs depending on epitope targeted as compared to solo control IgG or self-paired Ab preinjection. (C) Preadministration of paired Ab_{1m} (20 nM) enhances lung uptake of Ab_{2m}/NCs with different targeted antibody density on the particle surface (i.e., no. of Abs per particle) as compared to solo IgG. (D) Collaborative enhancement of Ab_{2m}/NC lung uptake with paired Abs, presented as percent solo lung uptake, decreases with increased NC avidity. Data are reported as the mean ± SE (n = 3−9 mice per group). ***, $P < 0.001$, n.s., $P > 0.05$. Hashed, filled, and open bars show NC binding with paired Ab, self-paired Ab, or solo IgG treatment, respectively.

here that Ab_{1h} had no effect on binding of Ab_{2h}/NC, regardless of the presence of flow (Figure 2B). While these results are somewhat counterintuitive, since Ab_{2h}/NC generally displays less effective solo binding than Ab_{1h}/NC (thereby providing "more room" for stimulation), clearly the stimulatory effects of paired Abs are epitope dependent and, for the time being, must be determined empirically.

***In Vivo* Ab/NC Targeting to Mouse Pulmonary Vasculature Is Enhanced with Paired Antibody.** To examine the ultimate physiological relevance and potential medical utility of these *in vitro* findings we recapitulated them *in vivo*. The pulmonary vasculature, with its privileged perfusion, extended endothelial surface area,[38] and high PECAM expression levels (up to 10^6 copies per cell),[39,40] is the preferential site of accumulation of PECAM-targeted agents.[41−44] Accordingly, we studied effects of preadministration of self-and paired PECAM antibodies on the pulmonary accumulation of radiolabeled Ab/NC injected in naïve mice, by determining percent injected dose per gram of lung tissue (%ID/g) following intravenous (IV) injection.

Ab_{1m}/^{125}I-NC injected "solo" accumulated in the pulmonary vasculature due to specific PECAM targeting, in contrast with control IgG/NC (Figure 4A). Injection of excess free "self" Ab_{1m} obliterated pulmonary accumulation of Ab_{1m}/^{125}I-NC to the level of nonspecific uptake of IgG/NC *via* the classical competitive inhibition paradigm. In stark contrast, paired Ab_{2m} enhanced the pulmonary uptake of Ab_{1m}/^{125}I-NC more than 5.4-fold relative to solo Ab/NC administration (Figure 5A, $P < 0.001$). Concomitantly, the blood level of Ab/NC was decreased in mice preinjected with the paired Ab relative to solo Ab/NC delivery, likely depleted in the blood pool due to more effective binding to the endothelium. This result establishes that collaborative enhancement of Ab/NC by paired antibodies does operate *in vivo* and enables almost an order of magnitude improvement in targeting. In fact, the effect exceeds that for free antibodies: Ab_{2m} caused markedly more modest, approximately 2-fold stimulation in the pulmonary uptake of ^{125}I-Ab_{1m} (Supporting Information, Figure S5A).[29] When lung uptake is corrected for nonspecific IgG/NC uptake, there is more than a 8.5-fold enhancement in Ab_{1m}/NC lung uptake following paired Ab_{2m} pretreatment *versus* solo treatment (Figure 5B).

Vice versa, paired Ab_{1m} similarly enhanced ^{125}I-Ab_{2m} lung uptake about 2-fold, whereas targeting was obliterated by unlabeled self-paired Ab injection to the level of nonspecific uptake of control IgG (Supporting Information, Figure S5B).[29] In this case, however, the nanocarrier effects did not mirror what was seen with the free antibody. Specifically, lung uptake of Ab_{2m}/^{125}I-NC was not significantly affected by paired Ab_{1m} when compared to solo binding (Figure 4B, Figure 5B).

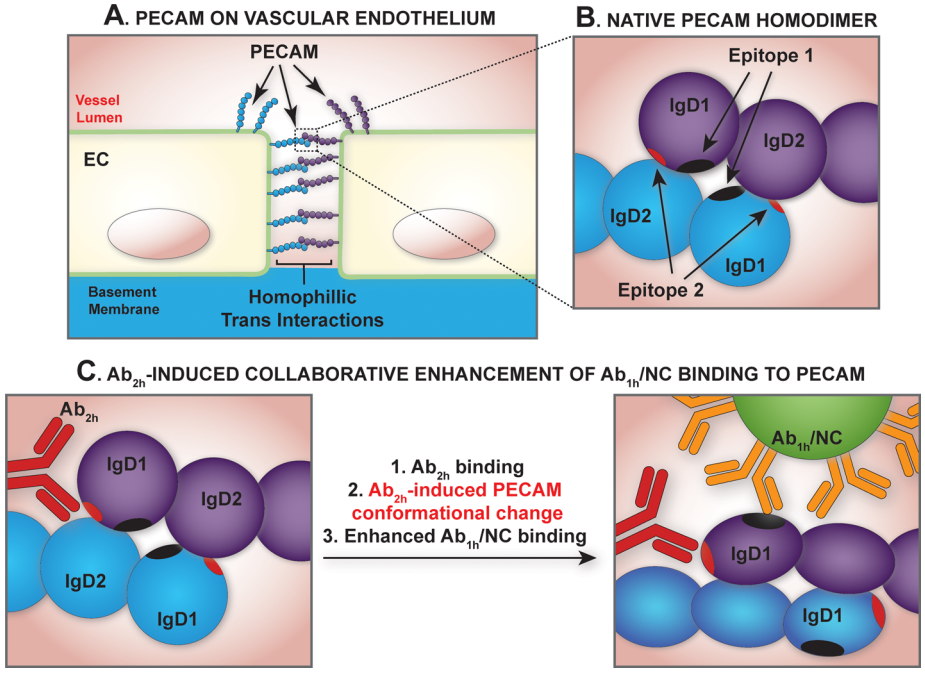

Figure 6. Hypothetical model of collaborative enhancement of anti-PECAM/NC binding with paired Ab. (A) PECAM expression on the vascular endothelium exists both in monomeric and trans-endothelial homodimeric forms. (B) Homodimeric binding is mediated by IgG domains 1 and 2 (IgD1 and IgD2), which bear epitopes of variable accessibility and affinity for respective Ab ligands, as depicted by the spherical and ellipsoidal shapes of IgD1 and IgD2. (C) The paired antibody Ab_{2h} increases the accessibility of a second distinct but paired PECAM epitope, such that Ab_{1h}/NC binding has increased.

Pulmonary accumulation of radiolabeled free Ab_{1m} was considerably higher than that of Ab_{2m}, which is likely due to the fact that Ab_{1m} has an order of magnitude higher affinity in contrast to Ab_{2m} (Supporting Information, Table S1). Notwithstanding this, Ab_{2m}/NC has higher lung uptake *versus* Ab_{1m}/NC; in other words, Ab_{2m}/NC accumulates in the lungs better, while Ab_{1m}/NC has worse lung uptake compared to their respective free antibodies. This opposing and unpredictable outcome can be attributed speculatively to elevated avidity of multivalent Ab_{2m}/NC and reduced accessibility of PECAM epitope to large Ab_{1m}/NC *versus* free antibody counterparts.

The innocuous effect of paired Ab_{1m} on particles carrying Ab_{2m} at high surface density is perhaps because the high avidity Ab_{2m}/NC engages enough PECAM copies to achieve maximal binding, even if the presence of paired Ab_{1m} exposes additional epitopes. To explore this, pulmonary uptake of Ab_{2m}/^{125}I-NC coated with 50 and 100 Abs per particle with solo and Ab_{1m} pretreatment was examined. As expected, the absolute amplitude of targeting efficiency decreased with reducing Ab coating surface density (Figure 5C), reflecting reduced avidity of the Ab/NC toward the Ab_{2m}-targeted PECAM epitope. However, reduction of Ab_{2m}/NC avidity indeed unveils significant collaborative enhancement by free paired Ab_{1m}. When corrected for IgG/NC lung uptake, lower avidity nanocarriers with 50 Ab per NC have greater than 5.5-fold increase in lung targeting specificity with paired Ab pretreatment compared to solo binding (Figure 5D). Paired Ab_{1m} presumably exposes more of the Ab_{2m} epitope, and this effect of collaborative enhancement stimulated lung uptake of Ab_{2m}/NC, which was only significantly enhanced when antibody coverage for Ab_{2m}/NC was <100 Abs per NC (i.e., avidity was suboptimal).

The current report demonstrates for the first time the enhancement of nanoparticle binding to surface motifs by modulating the target using paired antibodies to adjacent epitopes at the membrane surface. Figure 6 illustrates our hypothetical model of collaborative enhancement with PECAM-targeted reagents. The model, which borrows conceptually from protein allosteric modulation by ligand-induced protein conformational changes, takes into account the observation that a modulating antibody, assigned here as Ab_{2h} accessible to epitope 2, when incubated with live cells *in vitro* or injected *in vivo*, increases the accessibility of a second distinct but paired PECAM epitope 1, such that Ab_{1h}/NC binding has increased. Vascular PECAM exists in monomeric form in sensor domains in the plasmalemma and as is concentrated at EC intercellular junctions in trans−trans homophilic dimers (Figure 6A,B). The binding of a paired ligand may cause conformational changes in PECAM making the second epitope more accessible, which may be especially important for improving the binding of Ab/NC—large entities that require multivalent anchoring (Figure 6C).

While our findings are clearly relevant for pulmonary drug delivery, it is important to distinguish what specific

molecular mechanisms underlay the phenomenon of collaborative enhancement revealed for PECAM targeting, and whether or not it has generalizable features that extend to other targetable endothelial cell surface adhesion molecules. In this context, a systematic approach to mathematical modeling could be developed not only to describe the differential kinetics of targeted nanocarrier binding that result from induction of an augmentation of epitope accessibility but also to provide new physical insights for advancing modeling of multiparameter optimization in order to achieve safe and efficacious targeting in drug delivery applications. We have extensive experience in developing and implementing computational models of nanocarrier targeting to endothelium.[36,37,45] However, even the simplest modeling approaches intended to incorporate obvious factors impacting the design of functionalized therapeutic agents such as binding affinity, multivalancy, and *in vivo* targeting to endothelial cells require an extensive array of *in vitro* and/or *in vivo* experimental results for validation or data fitting. For example, to investigate the kinetic rate constants of nanocarrier attachment and detachment, critical information regarding receptor density, ligand density on the nanocarrier surface, and shear stress conditions were required before a temporal relationship between nanocarrier detachment rate and multivalent binding could be discerned.[46] Although the data from the present study, as well as those from our previous experiments,[29] are not sufficiently replete to enable us to populate a kinetic-based model describing the interplay between free and nanocarrier-bound antibodies, the findings we report are certainly consistent with the occurrence of molecular events through which binding of a particular antibody mediates the augmentation of subsequent binding of nanocarriers bearing another antibody. The facilitated exposure of the epitope participating in such collaboratively enhanced nanocarrier binding, as has been demonstrated herein both *in vitro* and *in vivo*, may occur through alterations in receptor conformation or orientation, emergence from sequestration within the glycocalyx or molecular spacing that confers a favorable thermodynamic profile for binding to occur. The challenge will be to demonstrate experimentally which of these, or other effects, is responsible for causing the collaborative enhancement we have described, in order to promote drug delivery applications to other potentially valuable targeting epitopes as well as to yield new modeling considerations for *in silico* discovery guided by careful investigational observation.

Interestingly, recent studies from other laboratories focused on mechanisms of PECAM signaling and adhesive function in leukocyte transmigration revealed that disruption of homophilic interactions between PECAM molecules in the endothelium by an Fab to PECAM IgD1 improved the binding of a second Fab to PECAM IgD6.[47] It is tempting to speculate that ligand-induced stepwise disassembly of PECAM "bunches" leading to exposure of more and more binding sites is involved in trans-cellular trafficking of leukocytes. In this context, Ab/NC of the present study might be viewed as an oversimplified model of a leukocyte. Unclear at this time is if the effect described herein is due to Ab-mediated disruption of homopohilic PECAM–PECAM interaction exposing more PECAM binding sites to the nanocarrier. This may not necessarily be the case since some of the stimulatory paired PECAM Abs (*i.e.*, Ab_{1h} and Ab_{2m}) employed in these studies are known to have no effect on trans-homophilic PECAM interactions. It is widely accepted that long-range conformational change is the mechanism of affinity modulation for members of the integrin,[48] cadherin,[49] and selectin[50,51] families, but there are only a few examples of this within Ig superfamily CAMs, most notably carcinoembryonic antigen (CEA)-related CAM 1 (CEACAM1),[52] Axonin 1[53] and the neural cell adhesion molecule L1.[54] Future structural studies are planned to examine the detailed conformational state of PECAM during antibody-mediated collaborative enhancement.

CONCLUSION

This paper represents the first attempt to define the role of the "collaborative enhancement" phenomenon in the vascular immunotargeting of nanocarriers *via* the cell adhesion molecule PECAM. Previously described with free anti-PECAM Abs and therapeutic fusion proteins, binding of a paired "stimulatory" ligand to one epitope can also lead to increased binding events of PECAM-targeted nanocarriers directed to a second distinct epitope. This study also showed the importance of epitope accessibility and avidity on endothelial targeting of nanocarriers. This paradigm offers a new approach for optimizing and enhancing the endothelial-targeted delivery of NC platforms carrying diverse therapeutic cargoes, from antithrombotic agents to antioxidants. Investigations are ongoing to improve understanding of the phenomena being reported.

METHODS

Materials. Fluorescein isothiocyanate (FITC)-labeled polystyrene spheres (~125 nm effective diameter) were purchased from Polysciences (Warrington, PA). ^{125}I-radiolabled poly(4-vinylphenol) nanoparticle spheres (~145 nm effective diameter) were prepared as previously described.[55,56] Purified monoclonal antibodies (mAbs) to human PECAM (huPECAM), clone 62 (mouse IgG2a, referred to as Ab_{1h}), and clone 37 (mouse IgG1, referred to as Ab_{2h}), were generously provided by Dr. M. Nakada (Centocor, Malvern, PA).[26] The antimouse PECAM (muPECAM) monoclonal antibody clones 390 (rat IgG2a, referred to as Ab_{1m})[57]

and MEC13.3 (rat IgG2a, referred to as Ab_{2m})[58] were purchased from BD Bioscience (Chicago, IL) and BioLegend (San Diego, CA), respectively. Nontargeted IgG Ab was an isotype mouse IgG (Jackson Immunoresearch Laboratories, West Grove, PA). Fluorescent secondary antibody to antihuPECAM were purchased from Invitrogen (Carlsbad, CA). ActinRed 555 reagent was purchased from Life Technologies (Norwalk, CT). Human umbilical vein endothelial cells (HUVECs) endogenously expressing native huPECAM were purchased from Lonza (Walkersville, MD) and maintained in EGM-2 media (Lonza) supplemented with 10% (v/v) fetal bovine serum (FBS).

Ab Coating of Nanocarriers. The polystyrene-based nanocarriers (NC or ^{125}I-NC) were coated with Abs using established adsorption techniques based on interactions between the hydrophobic domains on the surface of mAbs and the relatively hydrophobic NC. Abs (in aqueous buffered solution containing ≤0.09% sodium azide (NaN_3)) were added to a NC suspension in PBS, vigorously vortexed for 1 min, and then placed on a rotating shaker for 1 h at room temperature. Briefly, the Ab/NC mixture was centrifuged at 12000*g* for 3 min and the supernatant (unbound Abs) was separated from the NC pellet (with Abs bound). A saturating antibody density of the NC surface was ~200 Ab molecules/NC (~8000 Ab molecules/μm^2). For variable anti-PECAM coating densities, total antibody density was balanced to saturation with nontargeted IgG. Ab/NC formulations had hydrodynamic diameters ranging from 180 to 210 nm as measured by dynamic light scattering (DLS, BI-90 Plus Particle Sizer, Brookhaven Instruments, Brookhaven, NY).

Live-Cell Anti-PECAM/NC Binding Studies. A six-channel μ-microslide (Ibidi, Germany) connected to a variable-speed peristaltic pump (Rainin RP-1, Columbus, OH) with a media reservoir, was used to subject HUVEC monolayers to treatments under static incubation conditions or under acute fluid shear stress (4 dyn/cm^2, 30 min).[32] HUVECs were maintained in an incubation chamber at 37 °C in 5% CO_2/95% air, and starved overnight in endothelial basal medium containing 0.5% fetal bovine serum without supplements prior to experiments. Cells were preincubated with an Ab solution (paired, self-paired, or solo control IgG in Hank's Balanced Salt Solution (HBSS)) for 30 min. The pump reservoir was loaded with Ab/NC (2.0×10^9 NC/mL in HBSS), and cells then incubated or perfused for 30 min. Thereafter, cells were washed extensively with HBSS to remove unbound particles, and cells were fixed with 1% paraformaldehyde (PFA) for 10 min for subsequent fluorescent staining and analysis. In studies examining the effect of endocytosis blockade on Ab/NC binding, HUVECs were preincubated with 5 mM sodium azide (NaN_3)/5 mM 2-deoxyglucose (2-DG) for 30 min or prefixed with 1% paraformaldehyde (PFA) for 10 min before incubating with free Abs or perfusing with Ab/NCs.

Microscopy and Quantification of Cell-Bound Anti-PECAM/NCs. PFA-fixed cells were treated and analyzed as previously described.[32] Briefly, washed cells were mounted with ProLong Antifade reagent with DAPI (Molecular Probes, Eugene OR) for subsequent fluorescence microscopy. Slides were imaged using an Olympus IX70 inverted fluorescence microscope, 40× PlanApo objectives and filters optimized for green fluorescence. Images were acquired using a Hamamatsu Orca-1 CCD camera and analyzed with ImagePro 3.0 imaging software (Media Cybernetics, Silver Spring, MD). For quantification, endothelial bound-immunobeads are scored automatically for total green fluorescent particles within an image field size of 10^4 μm^2. The data are shown as the mean of ≥6 images ± standard error (SE). Ab/NC binding with paired, self-paired, or solo control IgG pretreatment are shown as hashed bars, filled bars, or open bars, respectively, unless otherwise noted.

PECAM Distribution Studies. HUVEC were seeded in a polydimethylsiloxane flow chamber coated with fibronectin and grown until confluent. Once confluent, cells were exposed to either static conditions or fluid shear stress (5 dyn/cm^2) for 30 min or 12 h. Following cessation of flow, cells were fixed with 1% PFA, washed, and blocked with 3% BSA in HBSS prior to staining. PECAM staining was performed using Ab_{1h} at 1 μg/mL for 1 h at RT, followed by fluorescent antimouse secondary antibody. For F-actin staining, cells were permeabilized with 0.1% Triton X-100 for 5 min, washed, and treated with ActinRed 555 reagent per manufacturer protocol. Images were acquired using a Zeiss AxioObserver inverted microscope and analyzed using an open-source version of the ImageJ platform.

Biodistribution Studies. All animal studies were carried out in accordance with the Guide for the Care and Use of Laboratory Animals as adopted by the US National Institutes of Health and approved by the University of Pennsylvania IACUC. C57BL/6 female mice (18−22 g) were anesthetized and injected intravenously (IV) *via* jugular vein with unlabeled Ab (anti-PECAM or IgG, 30 μg/mouse). Following 30 min Ab pretreatment, the contralateral jugular vein was injected IV with approximately 2 μCi ^{125}I-Ab (0.2 μg) or Ab/^{125}I-NCs (0.2 mg) coated with anti-PECAM formulations or control IgG. All formulations were sterilized by passing through a 0.2 μM filter prior to injection. At 30 min postinjection (p.i.) of the radioligand, and tissues and organs (blood, lungs, heart, kidneys, liver, spleen, brain, and thyroid) were collected and weighed. Tissue radioactivity was measured in a γ-counter, and targeting parameters including percent of injected dose per gram of tissue (% ID/g) were calculated as previously described.[29] Data are reported as the mean ± SE of $n = 3-9$ mice per group.

Statistical Analysis. Results are expressed as mean ± SE unless otherwise noted. Significant differences between group means were determined using two-way ANOVA followed by *posthoc* Holm−Šídák multiple comparison test, with alpha = 5.0%.

Conflict of Interest: The authors declare no competing financial interest.

Acknowledgment. This work was supported by NIH R01-HL073940 (V.R.M.) and R01-HL087036 (V.R.M.), and U01-EB016027 (D.M.E./V.R.M.), and the support of NIH NRSA fellowship HL07954 (J.H.) through the Institute for Medicine and Engineering (P.F.D.).

Supporting Information Available: Supplemental figures and tables. The Supporting Information is available free of charge on the ACS Publications website at DOI: 10.1021/nn505672x.

REFERENCES AND NOTES

1. Cheng, Z.; Al Zaki, A.; Hui, J. Z.; Muzykantov, V. R.; Tsourkas, A. Multifunctional Nanoparticles: Cost *Versus* Benefit of Adding Targeting and Imaging Capabilities. *Science* **2012**, *338*, 903–910.
2. Howard, M.; Zern, B. J.; Anselmo, A. C.; Shuvaev, V. V.; Mitragotri, S.; Muzykantov, V. Vascular Targeting of Nanocarriers: Perplexing Aspects of the Seemingly Straightforward Paradigm. *ACS Nano* **2014**, *8*, 4100–4132.
3. Farokhzad, O. C.; Langer, R. Impact of Nanotechnology on Drug Delivery. *ACS Nano* **2009**, *3*, 16–20.
4. Langer, R. Drug Delivery and Targeting. *Nature* **1998**, *392*, 5–10.
5. Mane, V.; Muro, S. Biodistribution and Endocytosis of ICAM-1-Targeting Antibodies *Versus* Nanocarriers in the Gastrointestinal Tract in Mice. *Int. J. Nanomed.* **2012**, *7*, 4223–4237.
6. Ho, K.; Lapitsky, Y.; Shi, M.; Shoichet, M. S. Tunable Immunonanoparticle Binding to Cancer Cells: Thermodynamic Analysis of Targeted Drug Delivery Vehicles. *Soft Matter.* **2009**, *5*, 1074–1080.
7. Hong, S.; Leroueil, P. R.; Majoros, I. J.; Orr, B. G.; Baker, J. R., Jr.; Banaszak Holl, M. M. The Binding Avidity of a Nanoparticle-Based Multivalent Targeted Drug Delivery Platform. *Chem. Biol.* **2007**, *14*, 107–115.
8. Simone, E.; Ding, B. S.; Muzykantov, V. Targeted Delivery of Therapeutics to Endothelium. *Cell Tissue Res.* **2009**, *335*, 283–300.
9. Aird, W. C. Endothelium as a Therapeutic Target in Sepsis. *Curr. Drug Targets* **2007**, *8*, 501–507.
10. Ogawara, K.; Rots, M. G.; Kok, R. J.; Moorlag, H. E.; Van Loenen, A. M.; Meijer, D. K.; Haisma, H. J.; Molema, G. A Novel Strategy to Modify Adenovirus Tropism and Enhance Transgene Delivery to Activated Vascular Endothelial Cells *In Vitro* and *In Vivo*. *Hum. Gene Ther.* **2004**, *15*, 433–443.
11. Ding, B. S.; Hong, N.; Murciano, J. C.; Ganguly, K.; Gottstein, C.; Christofidou-Solomidou, M.; Albelda, S. M.; Fisher, A. B.;

Cines, D. B.; Muzykantov, V. R. Prophylactic Thrombolysis by Thrombin-Activated Latent Prourokinase Targeted to PECAM-1 in the Pulmonary Vasculature. *Blood* **2008**, *111*, 1999–2006.
12. Hajitou, A.; Trepel, M.; Lilley, C. E.; Soghomonyan, S.; Alauddin, M. M.; Marini, F. C., 3rd; Restel, B. H.; Ozawa, M. G.; Moya, C. A.; Rangel, R.; et al. A Hybrid Vector for Ligand-Directed Tumor Targeting and Molecular Imaging. *Cell* **2006**, *125*, 385–398.
13. Oh, P.; Li, Y.; Yu, J.; Durr, E.; Krasinska, K. M.; Carver, L. A.; Testa, J. E.; Schnitzer, J. E. Subtractive Proteomic Mapping of the Endothelial Surface in Lung and Solid Tumours for Tissue-Specific Therapy. *Nature* **2004**, *429*, 629–635.
14. Lin, X.; Dean, D. A. Gene Therapy for ALI/ARDS. *Crit. Care Clin.* **2011**, *27*, 705–718.
15. Kee, P. H.; Kim, H.; Huang, S.; Laing, S. T.; Moody, M. R.; Vela, D.; Klegerman, M. E.; McPherson, D. D. Nitric Oxide Pretreatment Enhances Atheroma Component Highlighting *In Vivo* with Intercellular Adhesion Molecule-1-Targeted Echogenic Liposomes. *Ultrasound Med. Biol.* **2014**, *40*, 1167–1176.
16. Tripathy, S.; Vinokour, E.; McMahon, K. M.; Volpert, O. V.; Thaxton, C. S. High-Density Lipoprotein Nanoparticles Deliver RNAi to Endothelial Cells to Inhibit Angiogenesis. *Part. Part. Syst. Char.* **2014**, *13*, 1141–1150.
17. Muzykantov, V. R. Biomedical Aspects of Targeted Delivery of Drugs to Pulmonary Endothelium. *Expert Opin. Drug Delivery* **2005**, *2*, 909–926.
18. Hood, E. D.; Chorny, M.; Greineder, C. F.; I, S. A.; Levy, R. J.; Muzykantov, V. R. Endothelial Targeting of Nanocarriers Loaded with Antioxidant Enzymes for Protection against Vascular Oxidative Stress and Inflammation. *Biomaterials* **2014**, *35*, 3708–3715.
19. Howard, M. D.; Greineder, C. F.; Hood, E. D.; Muzykantov, V. R. Endothelial Targeting of Liposomes Encapsulating SOD/Catalase Mimetic EUK-134 Alleviates Acute Pulmonary Inflammation. *J. Controlled Release* **2014**, *177*, 34–41.
20. Howard, M. D.; Hood, E. D.; Greineder, C. F.; Alferiev, I. S.; Chorny, M.; Muzykantov, V. Targeting to Endothelial Cells Augments the Protective Effect of Novel Dual Bioactive Antioxidant/Anti-Inflammatory Nanoparticles. *Mol. Pharmaceutics* **2014**, *11*, 2262–2270.
21. Preissler, G.; Loehe, F.; Huff, I. V.; Ebersberger, U.; Shuvaev, V. V.; Bittmann, I.; Hermanns, I.; Kirkpatrick, J. C.; Fischer, K.; Eichhorn, M. E.; et al. Targeted Endothelial Delivery of Nanosized Catalase Immunoconjugates Protects Lung Grafts Donated after Cardiac Death. *Transplantation* **2011**, *92*, 380–387.
22. Albelda, S. M.; Oliver, P. D.; Romer, L. H.; Buck, C. A. EndoCAM: A Novel Endothelial Cell-Cell Adhesion Molecule. *J. Cell Biol.* **1990**, *110*, 1227–1237.
23. Albelda, S. M. Endothelial and Epithelial Cell Adhesion Molecules. *Am. J. Respir. Cell Mol. Biol.* **1991**, *4*, 195–203.
24. Muller, W. A.; Weigl, S. A.; Deng, X.; Phillips, D. M. PECAM-1 Is Required for Transendothelial Migration of Leukocytes. *J. Exp. Med.* **1993**, *178*, 449–460.
25. Newman, P. J. The Biology of PECAM-1. *J. Clin. Invest.* **1997**, *99*, 3–8.
26. Nakada, M. T.; Amin, K.; Christofidou-Solomidou, M.; O'Brien, C. D.; Sun, J.; Gurubhagavatula, I.; Heavner, G. A.; Taylor, A. H.; Paddock, C.; Sun, Q. H.; et al. Antibodies against the First Ig-Like Domain of Human Platelet Endothelial Cell Adhesion Molecule-1 (PECAM-1) That Inhibit PECAM-1-Dependent Homophilic Adhesion Block *In Vivo* Neutrophil Recruitment. *J. Immunol.* **2000**, *164*, 452–462.
27. Garnacho, C.; Albelda, S. M.; Muzykantov, V. R.; Muro, S. Differential Intra-Endothelial Delivery of Polymer Nanocarriers Targeted to Distinct PECAM-1 Epitopes. *J. Controlled Release* **2008**, *130*, 226–233.
28. Sun, Q. H.; DeLisser, H. M.; Zukowski, M. M.; Paddock, C.; Albelda, S. M.; Newman, P. J. Individually Distinct Ig Homology Domains in PECAM-1 Regulate Homophilic Binding and Modulate Receptor Affinity. *J. Biol. Chem.* **1996**, *271*, 11090–11098.
29. Chacko, A. M.; Nayak, M.; Greineder, C. F.; Delisser, H. M.; Muzykantov, V. R. Collaborative Enhancement of Antibody Binding to Distinct PECAM-1 Epitopes Modulates Endothelial Targeting. *PLoS One* **2012**, *7*, e34958.
30. Greineder, C. F.; Chacko, A. M.; Zaytsev, S.; Zern, B. J.; Carnemolla, R.; Hood, E. D.; Han, J.; Ding, B. S.; Esmon, C. T.; Muzykantov, V. R. Vascular Immunotargeting to Endothelial Determinant ICAM-1 Enables Optimal Partnering of Recombinant scFv-Thrombomodulin Fusion with Endogenous Cofactor. *PLoS One* **2013**, *8*, e80110.
31. Greineder, C. F.; Brenza, J. B.; Carnemolla, R.; Zaitsev, S.; Hood, E. D.; Pan, D. C.; Ding, B. S.; Esmon, C. T.; Chacko, A. M.; Muzykantov, V. R. Dual Targeting of Therapeutics to Endothelial Cells: Collaborative Enhancement of Delivery and Effect. *FASEB J.* **2015**, DOI: 10.1096/fj.15-271213.
32. Han, J.; Zern, B. J.; Shuvaev, V. V.; Davies, P. F.; Muro, S.; Muzykantov, V. Acute and Chronic Shear Stress Differently Regulate Endothelial Internalization of Nanocarriers Targeted to Platelet-Endothelial Cell Adhesion Molecule-1. *ACS Nano* **2012**, *6*, 8824–8836.
33. Calderon, A. J.; Muzykantov, V.; Muro, S.; Eckmann, D. M. Flow Dynamics, Binding and Detachment of Spherical Carriers Targeted to ICAM-1 on Endothelial Cells. *Biorheology* **2009**, *46*, 323–341.
34. Muro, S.; Koval, M.; Muzykantov, V. Endothelial Endocytic Pathways: Gates for Vascular Drug Delivery. *Curr. Vasc. Pharmacol.* **2004**, *2*, 281–299.
35. Muro, S.; Wiewrodt, R.; Thomas, A.; Koniaris, L.; Albelda, S. M.; Muzykantov, V. R.; Koval, M. A Novel Endocytic Pathway Induced by Clustering Endothelial ICAM-1 or PECAM-1. *J. Cell Sci.* **2003**, *116*, 1599–1609.
36. Liu, J.; Weller, G. E.; Zern, B.; Ayyaswamy, P. S.; Eckmann, D. M.; Muzykantov, V. R.; Radhakrishnan, R. Computational Model for Nanocarrier Binding to Endothelium Validated Using *In Vivo*, *In Vitro*, and Atomic Force Microscopy Experiments. *Proc. Natl. Acad. Sci. U. S. A.* **2010**, *107*, 16530–16535.
37. Liu, J.; Agrawal, N. J.; Calderon, A.; Ayyaswamy, P. S.; Eckmann, D. M.; Radhakrishnan, R. Multivalent Binding of Nanocarrier to Endothelial Cells under Shear Flow. *Biophys. J.* **2011**, *101*, 319–326.
38. Stan, R. V. Anatomy of the Pulmonary Endothelium. In *The Pulmonary Endothelium: Function in Health and Disease*; Voelkel, N. F., Rounds, S., Eds.; John Wiley & Sons, Ltd: Chichester, UK, 2009; pp 25−32.
39. Newman, P. J. The Role of PECAM-1 in Vascular Cell Biology. *Ann. N. Y. Acad. Sci.* **1994**, *714*, 165–174.
40. Muro, S.; Muzykantov, V. R. Targeting of Antioxidant and Anti-Thrombotic Drugs to Endothelial Cell Adhesion Molecules. *Curr. Pharm. Des.* **2005**, *11*, 2383–2401.
41. Muzykantov, V. R.; Christofidou-Solomidou, M.; Balyasnikova, I.; Harshaw, D. W.; Schultz, L.; Fisher, A. B.; Albelda, S. M. Streptavidin Facilitates Internalization and Pulmonary Targeting of an Anti-Endothelial Cell Antibody (Platelet-Endothelial Cell Adhesion Molecule 1): A Strategy for Vascular Immunotargeting of Drugs. *Proc. Natl. Acad. Sci. U. S. A.* **1999**, *96*, 2379–2384.
42. Li, S.; Tan, Y.; Virooncharapan, E.; Pitt, B. R.; Huang, L. Targeted Gene Delivery to Pulmonary Endothelium by Anti-PECAM Antibody. *Am. J. Physiol. Lung Cell. Mol. Physiol.* **2000**, *278*, L504–L511.
43. Ding, B. S.; Gottstein, C.; Grunow, A.; Kuo, A.; Ganguly, K.; Albelda, S. M.; Cines, D. B.; Muzykantov, V. R. Endothelial Targeting of a Recombinant Construct Fusing a PECAM-1 Single-Chain Variable Antibody Fragment (scFv) with Prourokinase Facilitates Prophylactic Thrombolysis in the Pulmonary Vasculature. *Blood* **2005**, *106*, 4191–4198.
44. Scherpereel, A.; Rome, J. J.; Wiewrodt, R.; Watkins, S. C.; Harshaw, D. W.; Alder, S.; Christofidou-Solomidou, M.; Haut, E.; Murciano, J. C.; Nakada, M.; et al. Platelet-Endothelial Cell Adhesion Molecule-1-Directed Immunotargeting to Cardiopulmonary Vasculature. *J. Pharmacol. Exp. Ther.* **2002**, *300*, 777–786.
45. Liu, J.; Bradley, R.; Eckmann, D. M.; Ayyaswamy, P. S.; Radhakrishnan, R. Multiscale Modeling of Functionalized

Nanocarriers in Targeted Drug Delivery. *Curr. Nanosci* **2011**, *7*, 727–735.
46. Haun, J. B.; Hammer, D. A. Quantifying Nanoparticle Adhesion Mediated by Specific Molecular Interactions. *Langmuir* **2008**, *24*, 8821–8832.
47. Mei, H.; Campbell, J. M.; Paddock, C. M.; Lertkiatmongkol, P.; Mosesson, M. W.; Albrecht, R.; Newman, P. J. Regulation of Endothelial Cell Barrier Function by Antibody-Driven Affinity Modulation of Platelet Endothelial Cell Adhesion Molecule-1 (PECAM-1). *J. Biol. Chem.* **2014**, *289*, 20836–20844.
48. Luo, B. H.; Carman, C. V.; Springer, T. A. Structural Basis of Integrin Regulation and Signaling. *Annu. Rev. Immunol.* **2007**, *25*, 619–647.
49. Shi, Q.; Maruthamuthu, V.; Li, F.; Leckband, D. Allosteric Cross Talk between Cadherin Extracellular Domains. *Biophys. J.* **2010**, *99*, 95–104.
50. Waldron, T. T.; Springer, T. A. Transmission of Allostery through the Lectin Domain in Selectin-Mediated Cell Adhesion. *Proc. Natl. Acad. Sci. U. S. A.* **2009**, *106*, 85–90.
51. Lu, S.; Zhang, Y.; Long, M. Visualization of Allostery in P-Selectin Lectin Domain Using MD Simulations. *PLoS One* **2010**, *5*, e15417.
52. Klaile, E.; Vorontsova, O.; Sigmundsson, K.; Muller, M. M.; Singer, B. B.; Ofverstedt, L. G.; Svensson, S.; Skoglund, U.; Obrink, B. The CEACAM1 N-Terminal Ig Domain Mediates Cis- and Trans-Binding and Is Essential for Allosteric Rearrangements of CEACAM1 Microclusters. *J. Cell Biol.* **2009**, *187*, 553–567.
53. Freigang, J.; Proba, K.; Leder, L.; Diederichs, K.; Sonderegger, P.; Welte, W. The Crystal Structure of the Ligand Binding Module of Axonin-1/TAG-1 Suggests a Zipper Mechanism for Neural Cell Adhesion. *Cell* **2000**, *101*, 425–433.
54. Arevalo, E.; Shanmugasundararaj, S.; Wilkemeyer, M. F.; Dou, X.; Chen, S.; Charness, M. E.; Miller, K. W. An Alcohol Binding Site on the Neural Cell Adhesion Molecule L1. *Proc. Natl. Acad. Sci. U. S. A.* **2008**, *105*, 371–375.
55. Zern, B. J.; Chacko, A. M.; Liu, J.; Greineder, C. F.; Blankemeyer, E. R.; Radhakrishnan, R.; Muzykantov, V. Reduction of Nanoparticle Avidity Enhances the Selectivity of Vascular Targeting and PET Detection of Pulmonary Inflammation. *ACS Nano* **2013**, *7*, 2461–2469.
56. Simone, E. A.; Zern, B. J.; Chacko, A. M.; Mikitsh, J. L.; Blankemeyer, E. R.; Muro, S.; Stan, R. V.; Muzykantov, V. R. Endothelial Targeting of Polymeric Nanoparticles Stably Labeled with the PET Imaging Radioisotope Iodine-124. *Biomaterials* **2012**, *33*, 5406–5413.
57. Christofidou-Solomidou, M.; Nakada, M. T.; Williams, J.; Muller, W. A.; DeLisser, H. M. Neutrophil Platelet Endothelial Cell Adhesion Molecule-1 Participates in Neutrophil Recruitment at Inflammatory Sites and Is Down-Regulated after Leukocyte Extravasation. *J. Immunol.* **1997**, *158*, 4872–4878.
58. Vecchi, A.; Garlanda, C.; Lampugnani, M. G.; Resnati, M.; Matteucci, C.; Stoppacciaro, A.; Schnurch, H.; Risau, W.; Ruco, L.; Mantovani, A.; et al. Monoclonal Antibodies Specific for Endothelial Cells of Mouse Blood Vessels. Their Application in the Identification of Adult and Embryonic Endothelium. *Eur. J. Cell Biol.* **1994**, *63*, 247–254.